

Effect of f-SWCNT on the structure, electrical and optical properties of PANI thin films

TARIQ J. ALWAN*, ZAIN A. MUHAMMAD

Physics Department, College of Education, Al-Mustansiriyah University, Baghdad, Iraq

Polyaniline (PANI) and PANI/f-SWCNT thin films have been synthesized by a chemical oxidative polymerization method. Ammonium persulfate ($(\text{NH}_4)_2\text{S}_2\text{O}_8$) and hydrochloric acid (HCL) were used as an oxidizing agent and protonic acid dopant respectively. The results of XRD pattern showed that the neat PANI and PANI/f-SWCNT thin films have an amorphous structure with a broad diffraction peak around $2\theta = 25^\circ$ and $2\theta = 23^\circ$ respectively. FESEM images showed that both neat PANI and PANI/f-SWCNT thin films have nanorod structures and the diameter of PANI nanorod is about 95.8 nm. Also it is revealed that the aniline monomer was polymerized on the surfaces of f-SWCNT that leads to increase the nanorod diameters which become in the range of 100-195 nm. The conductivity measurements revealed that the value of percolation threshold (PT) was about 0.39 W% and the conductivity value of neat PANI is increased after incorporating f-SWCNT in PANI matrix. The value of direct allowed transition energy gap of neat PANI was 2.56 eV and it is decreased significantly after adding f-SWCNT to it. FTIR spectrum shows several absorption peaks centred at around 1556, 692, 1235, 830, 1450 and 1280 cm^{-1} which consider the characteristic band peaks of polyaniline.

(Received January 30, 2020; accepted October 21, 2020)

Keywords: Conducting polymer, PANI/f-SWCNT thin films, In-situ polymerization method

1. Introduction

Polymers which are able to conducting electricity are called conjugated polymers that are inherently conducting ones. They can be used like the metallic conductors or semiconductors. The carrier mobility is a biggest difference between inorganic semiconductors and conducting polymers. Many years ago, carrier mobility was lower in conductive polymers due to disorder in the polymeric system [1]. For time being, this difference is reduced as a new conducting polymers are invented and modern processing methods are developed. Organic polymers often consist of two types of bonds, σ -bond and π -bond. The electrons that belong to σ -bond are not able to move along the backbone of molecular since the carbon atoms are bounded by covalent bonds, whilst The conjugated polymers contains π -electrons, which are formed by alternating single and double bonds, are delocalized and hence have ability to conduct electricity [2]. In general, conjugated polymers are insulators, or semiconducting when they are in the pristine state such as polyaniline, polyacetylenes and polythiophenes. The energy gap of which can be greater than 2 eV and their electrical conductivity is 10^{-10} to 10^{-8} S/cm. The doping process greatly increases the electric conductivities of such polymers even for very low level of doping (<1%), reaching several orders of magnitude up to ~ 0.1 S/cm. The conductivity of various polymers increases to ~ 0.1 – 10 kS/cm after successive doping of conducting polymers [3]. Among many conducting polymers the PANI is considered as the most promising one due to its unique electrical and optical properties, in addition, its preparation is relatively simple and has excellent environmental

stability. It is widely accepted that there are three redox forms of PANI: leucoemeraldine, emeraldine and pernigraniline, only one of PANI's forms whose ability to posses electric conductivity which is a protonated emeraldine form. It is known that polaronic structure of PANI-ES determines its electric conductivity. A wide variety of PANI applications has been explored, including solar cells, display devices, anticorrosion coatings and chemical sensors [6]. Single-walled carbon nanotube (SWCNT) comprises a one graphite sheet in the form of a tubular cylinder and has outstanding mechanical and electrical properties. SWCNT are used with many polyemers including polyaniline to form nanocomposites materials. CNT need to be distributed homogeneously in the polymer matrix in order to fabricate a nanocomposites of high-quality polymer-carbon with optimal performance [7]. The dispersion and alignment of CNT in the matrix is considered as a critical challenge in preparing a polymer-CNT composite with good processability characteristics, this challenge arises from the fact that the van der waal attraction among CNT often causes nanotubes to agglomerate. Hence, they can not readily dispersed in the polymer matrix. To overcome this problem, the Functionalisation by chemical reactions with extended molecular chains should be used [8]. The functionalized CNT should be readily dispersible in organic solvents and be more compatible with the polymer. The composites with chemical CNT bonds are much better than that mechanically mixed and have superior chemical and electrical properties [9]. Many of the previous studies prepared PANI/CNT thin films in different methods, Shalini Nagabooshanam et. al., 2020 [10] fabrication PANI/f-MWCNT thin films by electropolymerized

deposition and used for enzymatic detection of organophosphates. Weiyu Zhang et, al., 2020 [11] fabrication PANI/MWCNT film by coating the ceramic substrate with a layer of PANI/MWCNT paste using a thin brush to form gases sensing film. Rawat Jaisutti et, al., 2015 [12] prepared of PANi/MWCNT thin films by spin coating technique and used it for alcohol sensors. Samir Abdul Almohsin et, al., 2012 [13] also used electropolymerized method to deposition PANI/MWCNT thin films and investment in solar cell.

This paper presents the synthesis and characterization of PANI (ES) and PANI/f-SWCNT thin films prepared by in situ polymerization method. For enhancing SWCNT and PANI interface, chemical functionalization of SWCNT was used. The influence of f-SWCNT dopant concentration on the structural, optical and electrical properties of PANI was investigated.

2. Experimental

2.1. Functionalization of SWCNT

SWCNT was used as received. The concentrated H_2SO_4 and HNO_3 acids at ratio 3:1 were first utilized to treat ultrasonically one gram of SWCNT at $50\text{ }^\circ\text{C}$ for 4 h. These acids enhance the solubility of SWCNT in HCl solution and add to the defect sites some carboxylic acid groups. When the mixture has reached to room temperature by cooling process, it was centrifuged at 4000 rev/min in order to separate the treated SWCNT from mixture, then a filter paper with $0.22\text{ }\mu\text{m}$ porous was used for filtration. Deionized water was used to wash thoroughly the filtrated solid until the acid was removed completely. The filtered sample was placed in a furnace at $80\text{ }^\circ\text{C}$ for 6 h to dry. The final product was named as f-SWCNT.

2.2. Prepare PANI and PANI/f-SWCNT thin films

Aniline monomer, distilled water, ammonium persulfate (APS) and hydrochloric acid (HCL) were used as received. PANI was chemically synthesized by in-situ method by using aniline monomer and ammonium persulfate ($(NH_4)_2S_2O_8$) as oxidant agent. 1 M of HCL was placed in a 250 mL beaker, and during the polymerization process the beaker was kept inside a vessel containing an ice at a temperature of $(0-5)\text{ }^\circ\text{C}$. Separately, 50 mL of 1 M HCL was used to dissolve 15 g of APS which is added as dropwise into the beaker that contains the aniline acid solution for 5 min and under constant stirring. A couple of seconds later, the growth of polyaniline with a green color was observed and the color gradually spread into the aqueous solution which is changed its color into dark green within 5 min. The temperature of the reaction medium was maintained throughout this whole process at the range $(0-5)\text{ }^\circ\text{C}$.

PANI thin films were produced on glass slides. Prior to use the glasses, they washed with acetone and distilled water via ultrasonic. To cover only one side of the glass with PANI, an adhesive tape was adhered to the other side.

Using plastic clamps, the glasses was placed in the 250 ml beaker after mixing the aniline monomer and oxidant solutions, then all glasses taken out from the medium after 30 min from the start of reaction. It is observed that this is the best time to obtain uniform thin films. To confirm that the prepared thin films are all in the the emeraldine oxidation state (EOS), it was necessary to place the glasses again in a beaker which contains a solution of 2 ml aniline in 100 ml of 1 M HCL in order to reduce any polymer's oxidized pernigraniline form in EOS, at $(0-5)\text{ }^\circ\text{C}$ [14]. Afterwards, the precipitate of the adhering PANI was removed by washing the glasses with 1 M HCL, removed from the tape, washed with acetone ,and dried up at ambient temperature. For preparing PANI/f-SWCNT thin films, a different weight ratios of f-SWCNTs (0, 0.39, 0.5, 1, 1.5 and 2) W% were ultrasonicated in 50 ml of 1 M HCL for 30 min, then 5 ml of aniline monomer added to the solution under constant stirring for 30 min. At a reaction temperature of $(0-5)\text{ }^\circ\text{C}$ and constant stirring the APS was gradually poured dropwise into aniline/f-SWCNT solution for 3 min. The rest of procedure of obtained PANI/f-SWCNT thin films is similar to that of PANI thin films. The measured thicknesses of the films were about $(200\pm 20)\text{ nm}$. At normal incidence, spectrum of transmittance and absorbance in the range $(300-900)\text{ nm}$ were utilized to carry out the optical measurements of thin films prepared on glass slides, the type of UV-VIS spectrophotometer used is (SHIMADZU)(UV-1600/1700 series). FTIR analysis was carried out by using SIDCO England series FT-IR spectrometer over the range $650\text{ to }2500\text{ cm}^{-1}$. X-ray diffraction (XRD) of type (SHIMADZU-6000) was used to investigate the crystal structure of thin films , the Bragg's angle 2θ was recorded in the range $(10^\circ - 80^\circ)$ with the CuK_α source of wavelength $\lambda = 1.5406\text{ \AA}$. The field emission scanning electron microscopy (TESCAN- MIRA3 -FESEM) was used to observe surface morphology of prepared thin films.

3. Results and discussion

XRD was used to examine the crystallinity properties of the neat PANI and PANI/f-SWCNT thin films as shown in Fig. 1. The results show that the neat PANI sample

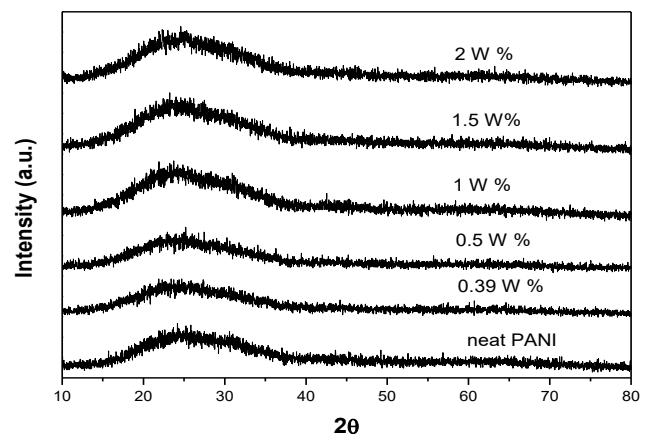


Fig. 1. XRD analysis of the neat PANI and PANI/f-SWCNT thin films

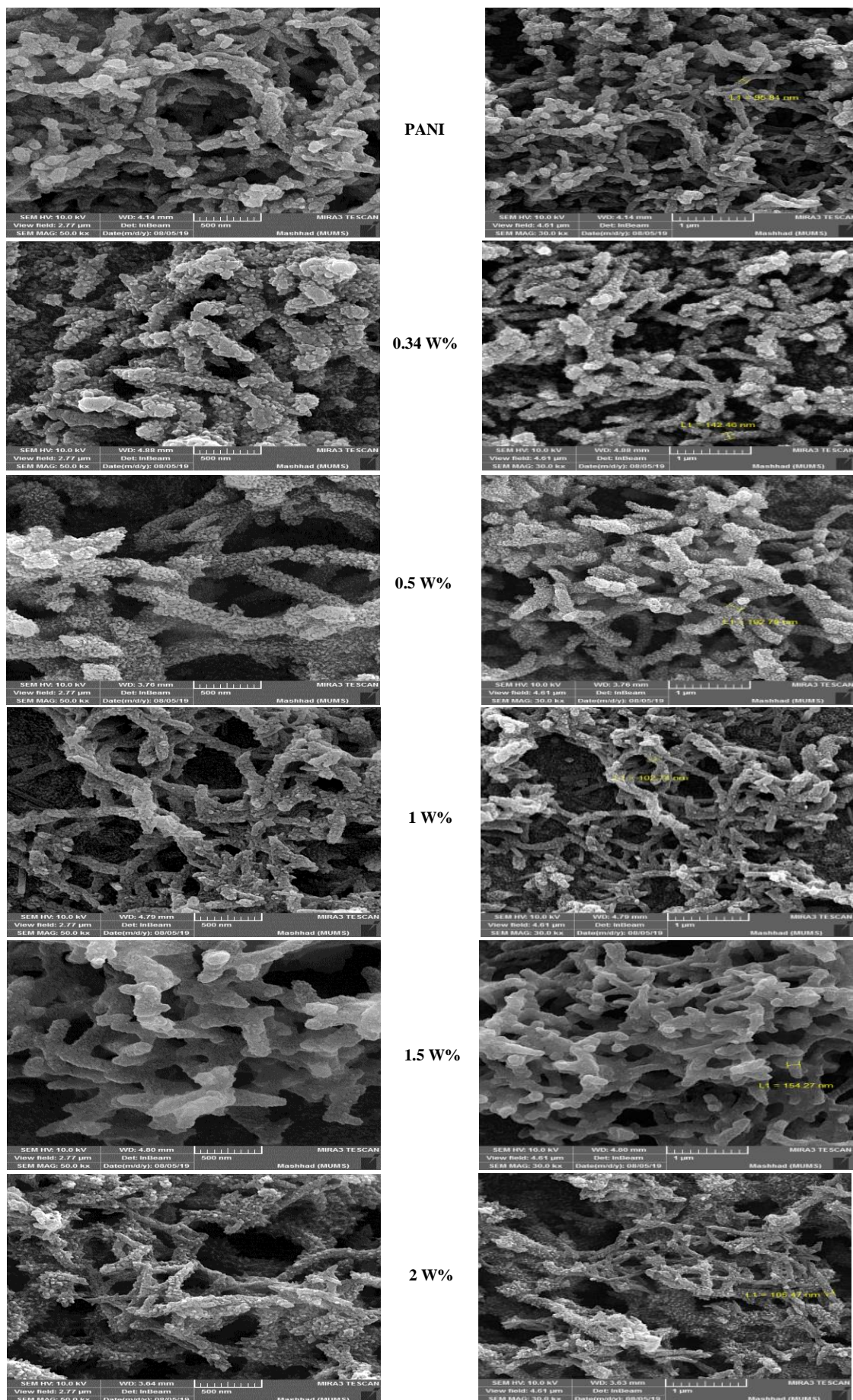


Fig. 2. FESEM images for the neat PANI and PANI/f-SWCNT thin films

is highly disordered with a broad diffraction peak around $2\theta = 25^\circ$. Also it can be seen that the observed XRD patterns of PANI/f-SWCNT thin films display an abroad peak around $2\theta = 23^\circ$. The latter observation suggest that the amorphous structure of the neat PANI are not altered by employing f-SWCNT in PANI matrix. The morphology of prepared samples was examined by an excellent technique which is FESEM. Fig. 2 shows FESEM images for the neat PANI and PANI/f-SWCNT thin films deposited on glass substrates at different weight ratios (W%) of f-SWCNTs and there are two scale bars 500 nm and $1\mu\text{m}$ for each image. It is clear from the images that the method of in situ oxidative polymerization is a suitable method to achieve a more homogeneous dispersion of f-SWCNT in polymer matrix. Closer inspection of the image of neat PANI, as shown in the image A, reveals that it contains nanorod structure and the surfaces of these nanorods are almost smooth, with the diameter is about 95.8 nm. After adding carbon nanotubes to PANI matrix, as shown in the images B, C, D, E and F, it is noted that the shapes of the nanorods begin to become clearer and separated from each other and their dispersion in the sample increase. In addition, The length and diameter of the nanorods start to increase, which become in the range of 100-195 nm. The surfaces of these nanorods become more roughness. This roughness is attributed to the aniline monomer that polymerized uniformly on the surface of the f-SWCNT and forms a tubular shell of PANI/f-SWCNT. These results are a good agreement with a literature [15]. Conductivity measurements were carried out on the neat PANI and PANI/f-SWCNT thin films using a two-point probe method. The values of the conductivity are given by the following equation:

$$\sigma = 1/\rho \quad (1)$$

where σ electrical conductivity and ρ resistivity SWCNT has a low critical concentration which is called as percolation threshold (PT). PT is defined as a minimum concentration required to make a conducting network within the host material [16]. The parameters on which PT depends are polymer type, nanotube type, tube size, synthesis method and dispersion method [17]. Fig. 3 shows that the obtained results indicate that as the W% of the f-SWCNT in the samples increases, the conductivity increases and reaches roughly a constant value after the concentration 0.5 W%, where the MWNTs dominate the electrical transport. PT is about 0.39 W% which agrees with a paper [16]. The values of the conductivity range from 2.95 S/cm for neat PANI to 7.31 S/cm for 0.5 W% as shown in the Table 1, this an increase provides a good indication that the incorporation of f-SWCNT into PANI was taken place. The increase of the free carrier density cause an increase in the conductivity. f-SWCNT may generate those free carries in PANI matrix and forms a conducting network that leads to an increase in the current [18].

Table 1. The conductivity and optical energy gap values at different W% of f-SWCNT %

f-SWCNTs (W %)	σ (300K) S/cm	E_g (eV)
0	2.95	2.58
0.39	5.40	2.58
0.5	7.31	2.58
1	7.26	2.58
1.5	7.19	2.56
2	7.30	2.49

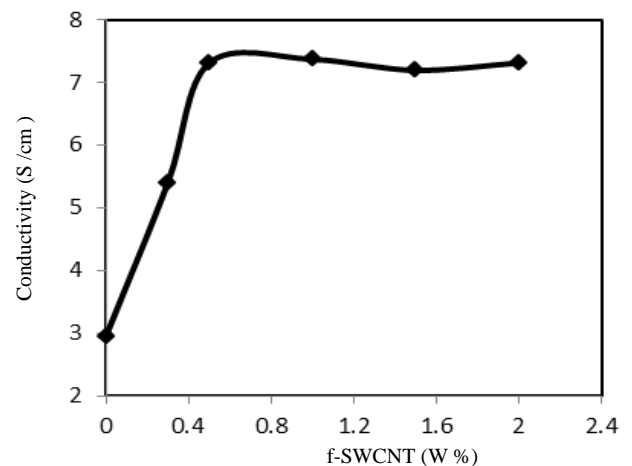


Fig. 3. The Conductivity of PANI and PANI/f-SWCNT thin films

Optical absorption spectra are considered one of the most important tools to compute the optical energy gap E_g of organic and inorganic semiconductors. The electrical conductivity and optical properties of PANI are specified by optical energy gap, so it is of fundamental importance. In many amorphous materials, it is found that the photon absorption can be calculated by Tauc relation [19], which is of the form:

$$\alpha h\nu = B (h\nu - E_g)^r$$

where α stands for the absorption coefficient, $h\nu$ represents photon energy, E_g is optical energy gap, B is a constant depending on the material's properties and r is a constant which can take various values that depends on the kind of electronic transition, for the direct and indirect allowed transition = 1/2 or 2, respectively. The best fit line is obtained for the direct allowed transition $r = 1/2$. Fig. 4 illustrates the $(\alpha h\nu)^2$ as a function of photon energy ($h\nu$) for direct allowed transition occurring in the neat PANI and PANI/f-SWCNT thin films. The optical energy gap are determined from this figure. It is observed that the optical energy gap of neat PANI is 2.58 eV and remains nearly the same at (0.39, 0.5 and 1) W% of f-SWCNT. However, it is decreased significantly to 2.56 eV and 2.49 eV at (1.5 and 2) W% of f-SWCNT respectively, as shown in the table 1. The decrease of optical band gap may be attribute to the interaction of f-SWCNT with PANI that gives rise

to the modification of the polymer structure [20]. To examine the molecules structure and their bonding, FTIR spectroscopy which is a suitable selection for both organic and inorganic materials was utilized. The unidentified elements present in the sample can also be identified. FTIR spectra of neat PANI and PANI/f-SWCNT thin films in the region of $(650-2500) \text{ cm}^{-1}$ were illustrated in Fig. 5. The characteristic band peaks for neat PANI occur at 1556, 692, 1235, 830, 1450 and 1280 cm^{-1} . The C=C stretch absorption of aromatic compound was obtained at 1556 cm^{-1} , the C-Cl stretching peak appears in the band peak 692 cm^{-1} confirmed the Cl- doping of the synthesized polyaniline films in HCL [21, 22]. The stretching of C-N $^+$ polaron structure appears at 1235 cm^{-1} which confirms the presence of conducting form of doped PANI

[23]. The band 832 cm^{-1} corresponding to aromatic ring out of plane deformation vibrations which belongs to C-H deformation in the para-disubstituted ring [24]. The band near 1450 cm^{-1} may be obscured by the aliphatic C-H deformation vibration, finally the band peak 1280 cm^{-1} is attributed to C-H plane bending, The characteristic peaks at 3422 cm^{-1} assigned to asymmetric N-H stretching vibration [25,26]. In comparison neat PANI spectra, the characteristic vibrational peaks of PANI are also appeared in the PANI/f-SWCNT thin films. FTIR spectra and the transmission peak intensities of PANI/f-SWCNT thin films are lower than that of pure PANI, indicating that the interaction between the f-SWCNT and the PANI matrix was taken place [27].

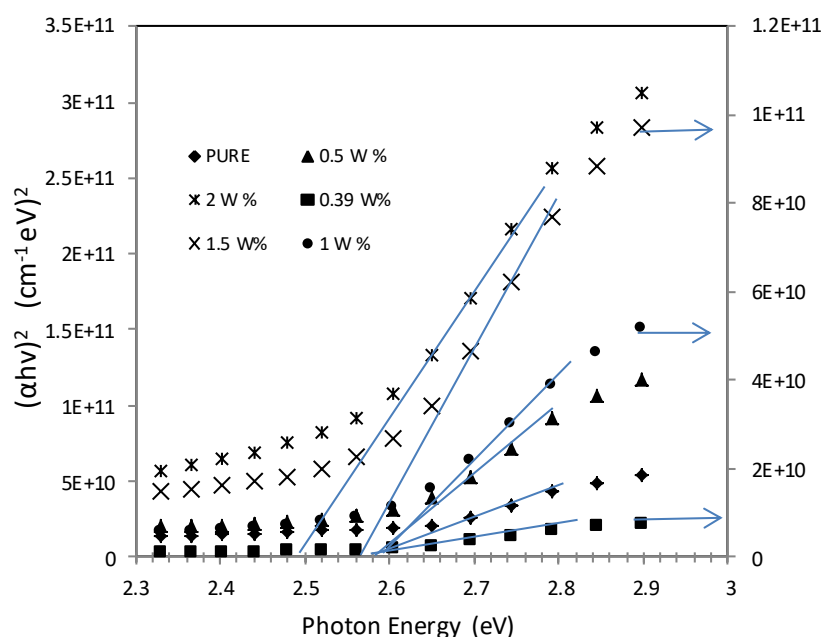


Fig. 4. The variation of $(\alpha hv)^2$ vs. (hv) for a neat PANI and PANI/f-SWCNT thin films

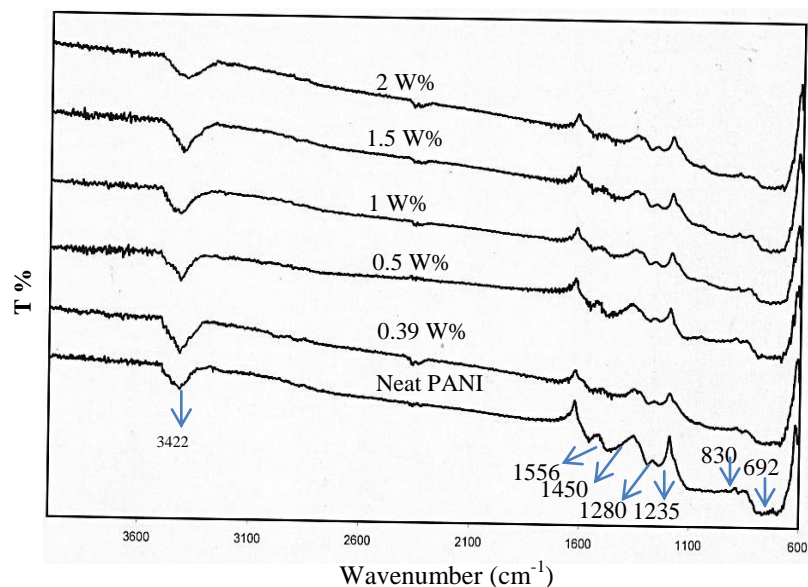


Fig. 5. FTIR spectra of PANI and PANI/f-SWCNT thin films

4. Conclusion

The neat PANI and PANI/f-SWCNT thin films are successfully deposited on a glass substrates by chemical oxidation polymerization technique. The XRD pattern revealed that the structure of neat PANI is an amorphous and not altered by adding f-SWCNT to its matrix. The FESEM images for neat PANI and PANI/f-SWCNT thin films showed that both have nanorod structures and the nanorod diameters of PANI/f-SWCNT thin films increased as result of polymerization PANI on the surface of f-SWCNT. The obtained value of PANI conductivity was 2.95 S/cm and turned out it is depend on the increase in W% of f-SWCNT that changed its conductivity to the roughly constant value of about 7.3 S/cm after 0.5 W%. The optical energy gap is effected by the addition of the f-SWCNT to PANI matrix, it was 2.58 eV for pure PANI sample and reduced to 2.49 eV for the 2 W% of f-SWCNT. FTIR measurement revealed the formation of PANI by displaying the characteristic band peaks belongs to it. The width and the intensity of the tansmission peaks are impacted by adding the f-SWCNT, indicating that the interaction between the f-SWCNT and the PANI matrix was taken place. The optical and electrical results indicated that neat PANI and PANI/f-SWCNT thin films are a semiconductor and can be used to fabricate optoelectronic devices.

References

- [1] M. Wan, *Conducting Polymers with Micro or Nanometer Structure*, Springer, 2008.
- [2] R. Hansson, *Materials and Device Engineering for Efficient and Stable Polymer Solar Cells*, Ph.D. Thesis, Karlstad Univ., Sweden, 2017.
- [3] M. T. Jaroslav Stejskal, Irina Sapurina, *Progress in Polymer Science* **35**(1), 1420 (2010).
- [4] G. X. Chaoqing Bian, Yijun Yu, *Journal of Applied Polymer Science* **116**(5), 2658 (2006).
- [5] R. Mažeikiene, V. Tomkute, Z. Kuodis, G. Niaura, and A. Malinauskas, *Vibrational Spectroscopy* **44**(2), 201 (2007).
- [6] E. Song, J.-W. Choi, *Nanomaterials* **3**(3), 498 (2013).
- [7] S. J. P. Min-Kang Seo, *Chemical Physics Letters* **395**, 44 (2004).
- [8] T. J. Alwan, *Optoelectron. Adv. Mat.* **13**(7-8), 472 (2019).
- [9] Y. Q. L. W. Fenga, X. D. Baib, *Carbon* **41**(2), 1551 (2003).
- [10] S. Nagabooshanam, A. T. John, S. Wadhwa, A. Mathur, S. Krishnamurthy, L. M. Bharadwa, *Food Chemistry* **323**, 126784 (2020).
- [11] W. Zhang, S. Cao, Z. Wu, M. Zhang, Y. Cao, J. Guo, F. Zhong, H. Duan, D. Jia, *Sensors* **20**, 149 (2020).
- [12] R. Jaisutti, K. Eaiprasertsak, T. Osotchan, *IEEE SENSORS Proceedings, Busan, South Korea*, 1-4 (2015).
- [13] S. Abdulalmohsin, Z. Li, Muatez M., K. Wu, J. Cui, *Synthetic Metals* **162**, 931 (2012).
- [14] J. K. Avlyanov, J. Y. Josefowicz, A. G. MacDiarmid, *Synthetic Metals* **73**(3), 205 (1995).
- [15] F. Huang, E. Vanhaecke, D. Chen, *Catalysis Today* **150**(1-2), 71 (2010).
- [16] S. Abdulalmohsin, Z. Li, M. Mohammed, K. Wu, J. Cui, *Synth. Met.*, **162**(11-12), 931 (2012).
- [17] Qingli Zhang, Weijie Wang, Jianlin Li, Juanjuan Zhu, Lianjun Wang, Meifang Zhu, Wan Jiang, *Journal of Materials Chemistry C* **3**(39), 10715 (2013).
- [18] P. C. Ramamurthy, A. M. Malshe, W. R. Harrell, R. V. Gregory, K. McGuire, A. M. Rao, *Solid-State Electronics* **48**(10-11), 2019 (2004).
- [19] K. Gupta, P. C. Jana, A. K. Meikap, *Synthetic Metals* **160**(1), 1566 (2010).
- [20] Y. Long, Z. Chen, X. Zhang, J. Zhang, Z. Liu, *Applied Physics Letters* **85**(1), 1796 (2004).
- [21] A. M. P. Hussain, A. Kumar, *Bulletin of Materials Science* **26**(3), 329 (2003).
- [22] C. K. Maity, S. Sahoo, K. Verma, A. K. Behera, G. C. Nayak, *New J. Chem.* **44**, 8106 (2020).
- [23] E. C. Gomes, M. A. S. Oliveira, *American Journal of Polymer Science* **2**(2), 5 (2012).
- [24] X. R. Zeng, T. M. Ko, *Polymer* **39**(5), 1187 (1998).
- [25] G. Socrates, *Infrared and Raman Characteristic Group Frequencies. Tables and charts*, 3rd ed. (2001).
- [26] T. J. Alwan, F. S. Jalli, *Optoelectron. Adv. Mat.* **12**(1-2), 100 (2018).
- [27] C. Dhand, S. K. Arya, S. Pal, B. Pratap, M. Datta, B. D. Malhotra, *Carbon* **46**, 1727 (2008).

*Corresponding author: tariqjaffer2000@yahoo.com